Carbohydrate Polymers 103 (2014) 285–293

Contents lists available at ScienceDirect

Carbohydrate Polymers

journal homepage: www.elsevier.com/locate/carbpol

Synthesis of starch-*g*-p(DMDAAC) using HRP initiation and the correlation of its structure and sludge dewaterability

Shenghua Lv*, Ting Sun, Qingfang Zhou, Jingjing Liu, Huaidong Ding

College of Resource and Environment, Shaanxi University of Science & Technology, Xi'an 710021, China

ARTICLE INFO

Article history:
Received 6 November 2013
Received in revised form
11 December 2013
Accepted 12 December 2013
Available online 19 December 2013

Keywords:
Cationic starch
Horseradish peroxidase
Sewage sludge
Sludge dewatering

ABSTRACT

A new cationic starch used as a sludge dewatering agent was prepared by grafting copolymerization of degradation starch and dimethyldiallylammonium chloride (DMDAAC) using horseradish peroxidase/H_2O_2 initiation. Its chemical structure was characterized by FTIR, ^{1}H NMR, ^{13}C NMR, gel permeation chromatography, graft percent, and graft efficiency. The results indicated that its structure was built by grafting the DMDAAC oligomer onto the starch backbone as branched chains, with stronger hydrophobic regions and higher cationic degree. The specific resistance of the filtration and capillary suction time of the sludge conditioned with the cationic starch decreased distinctly, and the sludge water content could be reduced to 50.6% from 97.85%. The dewatering mechanism is proposed based on the surface tension, zeta potential, and microstructure of sludge, which involves stronger hydrophobic regions and cationic groups producing a porous structure within the sludge. The research results may provide valuable ideas for developing high-performance sludge dewatering agents.

1. Introduction

In recent years in China, together with the increasing pace of urbanization and industrialization, huge amounts of sewage sludge have been produced in municipal sewage and industrial effluent treatment. The sewage sludge has a high water content (WC; 95–98%), and has the nature of a hydrogel with greater fluidity, resulting in it being more difficult to further treat and re-use. Sludge dehydration should therefore be the first task for sludge treatment, and the WC of the sludge should be reduced to below 60% so that it can be further processed. Although there are various types of sludge dewatering equipment available, dewatering agents are still indispensable additives in the sludge dewatering process (Ali, Aeyed, & Seyed, 2013; Pal, Sen, Karmakar, Mal, & Singh, 2008). The most common dewatering agents are anionic polyacrylate, nonionic polyacrylamide, and cationic polyacrylamide (CPAM) (Lin et al., 2012; Noppakundilograt, Nanakorn, Jinsart, & Kiatkamjornwong, 2010; O'Shea, Qiao, & Franks, 2011). These dewatering agents have poor dewaterability, and may produce secondary contamination. In addition, their synthetic raw materials mainly depend on petroleum resources and inevitably face the threat of resource exhaustion. Therefore, many researchers have recently focused on the use of natural polymers, such as starch and chitosan, as biodegradable, renewable, and cost-effective materials for the synthesis of flocculants. The development of cationic starch, especially suitable for sewage flocculation and sludge dewatering, has received considerable attention (Krentz et al., 2006; Ma, Zheng, Tan, Liu, & Chen, 2013; Mishra, Mukul, Sen, & Jha, 2011; Wang et al., 2012). Cationic starch may be prepared by etherification or graft copolymerization of starch and cationic monomers (Anthony & Sims, 2013). The cationic monomers used for etherification are mainly 3-chloro-2-hydroxypropyltrimethylammonium chloride (CTAC) or 2,3-epoxypropyltrimethylammonium chloride (ETAC) (Zou, Zhao, Ge, Lei, & Luo, 2012). The etherifying reaction is carried out between chlorine of CTAC or epoxy groups of ETAC and hydroxyl groups of starch. The cationic monomers are bonded to the starch skeleton to form branched chains. At present, studies have mainly focused on improving the dewaterability by increasing the degree of substitution and graft efficiency (Kavaliauskaite, Klimaviciute, & Zemaitaitis, 2008).

When cationic starch is prepared by grafting copolymerization, the cationic comonomers are diallyldimethylammonium chloride (DMDAAC) or 3-(methacryloylamino)propyltrimethylammonium chloride (Ochoa et al., 2007). DMDAAC alone cannot form a polymer due to its self-inhibition; generally, acrylamide (AM) is used as a comonomer to form a copolymer with DMDAAC. CPAM is actually a copolymer of AM and DMDAAC (p(AM-*co*-DMDAAC)). Therefore, cationic starch is actually p(AM-*co*-DMDAAC) grafted on the starch

* Corresponding author. Tel.: +86 029 86168291; fax: +86 029 86168291.
E-mail addresses: Lvsh@sust.edu.cn, lvsh630603@yahoo.com (S. Lv).

0144-8617/$ – see front matter © 2013 Elsevier Ltd. All rights reserved.
http://dx.doi.org/10.1016/j.carbpol.2013.12.036

skeleton to form starch-*g*-p(AM-*co*-DMDAAC). In recent years, improving the flocculation effect and dewaterability by increasing grafting percent (GP) and grafting efficiency (GE) using a suitable initiator has become a hot topic of research. Gamma irradiation and complex initiation by $Ce(SO_4)_2$–$K_2S_2O_8$ or $CO(NH_2)_2$–$(NH_4)_2S_2O_8$ have been investigated and have exhibited a significant effect (Lv et al., 2013).

The determination of the molecular structure of cationic starch is another difficult issue in this research field. Although there are many advanced structural measurement techniques, such as FTIR, NMR, and MS, its accurate molecular structure is still difficult to confirm due to the complexity of polymerization and the difficulty in separation of products. Nowadays, the molecular structure of cationic starch can usually be characterized by the FTIR, ^{1}H NMR, and ^{13}C NMR spectra of feature groups and structure (Randal & Shogren, 2013; Tawaki, Uchida, Maeda, & Ikeda, 2005).

Starch-*g*-p(AM-*co*-DMDAAC) has been used in sewage flocculation and exhibited a good flocculation effect and cost effectiveness (Pal, Sen, Karmakar, Mal, & Singh, 2008). However, using starch-*g*-p(AM-*co*-DMDAAC) as a sludge dewatering agent can lead to the sludge forming a sticky gel, meaning that the sludge WC cannot be reduced to below 60%. Therefore, improving the dewaterability of cationic starch has become an urgent and arduous task. The solution to this problem should be sought from the working mechanism of flocculation and sludge dewatering. Flocculation is a process of adsorption and bridging coagulation. The starch-*g*-p(AM-*co*-DMDAAC) with long molecular chains and strong cationic groups could produce strong adsorption and coagulation, so it has stronger flocculation effects in sewage treatment. Sludge dewatering is a process of water repelling and drainage, which differs distinctly from that of sewage flocculation. Formation of hydrophobic regions within the sludge and further development into a porous structure in a mechanical dehydrating process is the main feature of the mechanism. The hydrophobic regions and porous structure are the synergetic result of hydrophilic/hydrophobic regions and cationic groups. Therefore, the ideal sludge dewatering agent has not only hydrophilic groups for solubility and dispersion, but also stronger hydrophobic groups for forming the hydrophobic regions for building drainage channels. In starch-*g*-p(AM-*co*-DMDAAC), the hydrophobic groups and cationic groups are separated by hydrophilic nonionic AM units, so the hydrophobic groups cannot connect to form hydrophobic regions. Therefore, the self-structure of starch-*g*-p(AM-*co*-DMDAAC) leads to its poor dewatering capacity.

Based on the analysis above, a new cationic starch with an ideal molecular structure for sludge dehydration was designed and prepared by grafting oligomeric p(DMDAAC) onto the starch skeleton using a horseradish peroxidase (HRP) initiation system. The oligomers are bonded to the starch as branched chains, which consist of five- or six-membered rings of DMDAAC. The ring-structure units connected directly may form large hydrophobic regions and strong cationic regions. This molecular structure is designed specifically for improving the sludge dewaterability of the cationic starch. The special structure can only be built by HRP initiation. HRP is a kind of enzyme-mediated initiator, its outstanding features being a unique initiation mechanism and structural controllability, as well as moderate reaction conditions and high reaction efficiency (Anthony & Sims, 2013; Lv, Gong, & Ma, 2012). The molecular structure was demonstrated by FTIR, ^{1}H NMR, and ^{13}C NMR spectroscopies. The sludge dewaterability was investigated using the specific resistance of filtration (SRF), capillary suction time (CST), and dewatering ratio of sludge. The working mechanism was probed by investigation of the surface tension, zeta potential, pore structure, and SEM images of the sludge.

2. Experimental

2.1. Materials

HRP, with an activity of 2900 U mg^{-1} and M_w of 3000, and thermostable α-amylase, with an activity of 10,000 U mg^{-1} and maximum suitable temperature of 94 °C, were bought from Beijing Biosynthesis Biotechnology Company (Beijing, China). Cornstarch was supplied by the Xi'an Starch Factory (Xi'an, China). Hydrogen peroxide (H_2O_2, 30 wt%), DMDAAC, sodium bicarbonate ($NaHCO_3$), toluidine blue indicator, potassium polyvinyl sulfate (PVSK), and methanol were supplied by the Xi'an Chemical Reagent Factory (Xi'an, China).

The municipal sewage and sludge came from the aerated grit chambers and secondary settling tanks, respectively, of urban sewage treatment plants (Xi'an, China). The important parameters of the sewage sludge were as follows: pH 7.53; zeta potential, −24.3 mV; SRF, 7.53×10^{13} m kg^{-1}; CST, 76.53 s; water content, 97.85%; total solids, 2.15%; organic matter, 53.6% dry basis; total nitrogen content, 2.79% dry basis; and total phosphorus, 2.61% dry basis.

The control samples were CPAM and starch-*g*-p(AM-*co*-DMDAAC). CPAM was prepared by copolymerization of 20 g of AM and 15 g of DMDAAC using $(NH_3)_2S_2O_8$ initiation. The cationic degree (CD) was 41.5%. The M_w and M_n were 85,427 and 72,395, respectively. Starch-*g*-p(AM-*co*-DMDAAC) was synthesized by graft copolymerization of 10 g of starch, 10 g of AM, and 19 g of DMDAAC using $Ce(SO_4)_2$–$K_2S_2O_8$ initiation. The CD was 39.4%, and M_w and M_n were 164,562 and 127,567, respectively.

2.2. Preparation of starch-g-p(DMDAAC)

Amounts of 25 g of starch and 0.01 g of thermostable α-amylase were placed into a three-neck round-bottom flask with 75 g of deionized water under stirring. Then, the mixture was heated and kept at 90 °C for 2 h. This was then cooled to 35 °C, with the product being degraded starch. Then, 25 g of DMDAAC was added to the degraded starch solution and the pH value adjusted to 7.0 with $NaHCO_3$, with the temperature being kept at 45 °C. Then, a certain amount of HRP was added at once, and H_2O_2 was added dropwise for 1 h. After adding the H_2O_2, the reaction was continued at 45 °C for 6 h. The final product was starch-*g*-p(DMDAAC).

2.3. Structural characterization of starch-g-p(DMDAAC)

2.3.1. FTIR and NMR spectra

FTIR spectra were obtained using an EQUINOX-55 FTIR spectrometer (Bruker, Germany). The samples were purified by precipitation and washing with methanol.

The ^{1}H NMR and ^{13}C NMR spectra were obtained using an INOVA 400 MHz spectrometer (AVANCE III, Switzerland). The samples were purified, dried, and then dissolved in deuterated dimethyl sulfoxide (DMSO).

2.3.2. Gel permeation chromatography

M_w, M_n, and polydispersity index (PDI) were measured using a gel permeation chromatograph (model 2414, Waters, USA). Sodium azide solution (0.10 mol L^{-1}) was utilized as the carrying phase at a flow rate of 1 mL min^{-1} at 40 °C. The standard sample was poly(ethylene glycol). The samples were purified following the same procedure as before.

2.3.3. Cationic degree

The CD was determined by colloid titration. Cationic starch (0.02 g) was accurately weighed in a 250 mL Erlenmeyer flask with 100 mL of deionized water. Then, the solution pH value was

adjusted to 3 with diluted HCl solution (0.1 mol L^{-1}), and 2–3 drops of toluidine blue (0.1%) were added as an indicator. This was then titrated with PVSK standard solution (0.025 mol L^{-1}), with a purple color indicating the titration endpoint. This experiment was repeated three times, and the data averaged. The CD can be calculated from the following equation:

$$CD = \frac{161.5 \times 0.5 \times (V - V_0)}{1000\ m} \times 100\% \quad (1)$$

where V and V_0 are the volumes of PVSK standard solution-titrated samples and blank samples (mL), respectively, m is the mass of the sample, 161.5 is the molar mass of the cationic monomeric unit, and 0.5 is the molar concentration of the PVSK standard solution (mol L^{-1}).

2.3.4. Graft percent and graft efficiency

A purified sample was ground to a powder (W_1), then extracted for 12 h in a Soxhlet extractor using a mixture of acetone and glacial acetic acid (1:1, v/v), and ungrafted p(DMDAAC) and unreacted monomers were removed. The purified starch-*g*-p(DMDAAC) was dried at 100 °C to a constant weight (W_2). The masses of starch and DMDAAC are W_0 and W_m, respectively. GP and GE were calculated using the following equations:

$$GP = \frac{W_2}{W_0} \times 100\% \quad (2)$$

$$GE = \frac{W_2 - W_0}{W_m} \times 100\% \quad (3)$$

2.4. Sewage flocculation effect

The flocculation effect was evaluated by the turbidity removal ratio (TRR). An amount of 2000 g of sewage was placed into a 3000 mL beaker, and then a certain amount of starch-*g*-p(DMDAAC) was added and stirred for 1 min. Then, it was left to stand for solid/liquid separation. TRR was calculated using the following equation:

$$TRR = \frac{I_0 - I_1}{I_0} \times 100\% \quad (4)$$

where I_0 and I_1 are the absorbance of sewage and filtrate, respectively, which was obtained using a UV-1900 spectrophotometer (Shanghai, China).

2.5. Sludge dewaterability

The sludge dewaterability was evaluated in terms of SRF, CST, and WC of the sludge.

2.5.1. SRF and CST of sludge

SRF was determined by the Buchner funnel method (Lu, Lin, Liao, Huang, & Ting, 2003). CST was measured with a CST instrument (model 319, Triton Electronics Ltd, UK) equipped with an 18 mm diameter funnel and Whatman No. 17 chromatography-grade paper.

2.5.2. WC of sludge

A certain amount of starch-*g*-p(DMDAAC) was added to 200 g of sludge and stirred for 2 min. This was then transferred to a Buchner funnel and filtered at a vacuum suction of 0.1 MPa for 10 min. The WC and dewatering ratio (DR) of the sludge were obtained from the following equations:

$$WC = \frac{m_0 - m_1}{m_0} \times 100\% \quad (5)$$

$$DR = \frac{m_0 - m_1}{m_0 - m_2} \times 100\% \quad (6)$$

where m_0 and m_1 are the masses of the mud cake before and after filtering, respectively, and m_2 is the mass of the mud cake after drying at 105 °C for 2–3 h.

2.6. Investigation of the working mechanism

The dewatering mechanism of starch-*g*-p(DMDAAC) was probed by investigation of the surface tension of solution, the zeta potential of sludge, and the microstructure of the dewatered sludge in the presence of starch-*g*-p(DMDAAC).

2.6.1. Surface tension

The surface tension of solutions was tested using a JK99B automatic surface tension apparatus (Shanghai, China) at 25 °C. Sample solutions with different concentrations were obtained by diluting a solution of known concentration with distilled water. For each concentration, the measurement was repeated five times and an average taken.

2.6.2. Zeta potential

Original sewage sludge (10 g), 50 g of deionized water, and dewatering agent were mixed, and then 3 mL of the mixture was placed into an electrophoresis pool to measure the zeta potential using a JS94H microscopic electrophoresis instrument (Shanghai, China). Each sample was tested five times and the results averaged.

2.6.3. Microstructure of dewatered sludge

The microstructure of the dewatered sludge was characterized by the pore structure and from SEM images of the dewatered sludge.

The pore structure was measured using an Autopore® IV9500 automatic mercury porosimeter (Micromeritics Co. Ltd, USA). The samples were fragmented to about 10 mm × 10 mm × 5 mm and dried in a vacuum oven at 95 °C for 3 h. Then, the samples were accurately weighed and placed in an expansion joint and sealed. The measurement was implemented at low pressure (0–30 MPa) and high pressure (30–400 MPa) in sequence. The samples were reweighed before high-pressure testing. Each sample was tested three times and the results averaged.

SEM images of the dewatered sludge were obtained using a Hitachi S-4800 field emission scanning electron microscope (FESEM, Hitachi, Japan). The dried sludge cake was adhered on an aluminum stub and coated with gold by a sputter process for conductivity.

3. Results and discussion

3.1. Major factors affecting the properties of starch-g-p (DMDAAC)

The major factors affecting the properties of starch-*g*-p(DMDAAC) are the degradation degree of the starch, DMDAAC content, and HRP content, as discussed below.

3.1.1. Starch degradation degree

Native starch has a high molecular weight (MW) and strong intramolecular forces, resulting in its insolubility in water. Therefore, starch should be modified physically or chemically to improve its solubility and expand its usefulness (Kriz, Dybal, & Kurkova, 2002; Wang & Xie, 2010). The modification methods of the research involved enzyme degradation and graft copolymerization to improve the starch solubility and build a special molecular structure according to sludge dewatering requirements. The reason for

Table 1
Effects of degradation degree on properties of starch-*g*-p(DMDAAC).

Time (min)	Degradation degree (Da)			GP[a] (%)	GE[a] (%)	CD[a] (%)	TRR[b] (%)	WC[b] (%)	SRF[b] (10^{13} m kg^{-1})	CST[b] (s)
	M_n	M_w	PDI							
30	105,688	198,695	1.88	161.6	75.4	23.17	61.4	76.3	7.12	73.37
90	89,341	157,240	1.76	165.4	83.6	32.52	76.1	71.8	4.27	61.25
120	82,441	117,891	1.43	168.7	86.9	36.46	88.5	65.3	2.31	45.45
150	64,496	85,136	1.32	177.5	98.4	41.23	95.6	56.6	0.98	28.3
180	44,483	53,824	1.21	178.6	98.5	41.84	83.8	52.3	0.75	16.3
210	29,186	35,316	1.21	178.6	98.5	42.27	65.4	50.2	0.62	12.2
240	26,188	31,425	1.20	178.1	98.6	42.63	61.6	51.2	0.61	12.2

[a] Starch-*g*-p(DMDAAC) was prepared by graft polymerization of 25 g degraded starch and 25 g DMDAAC using HRP (12 mg)/H_2O_2 (15 mg) initiation at 45 °C for 6 h.
[b] The dosage was 0.6% by solid contaminant weight.

using enzyme degradation is that it has the advantages of simplicity, good yields, and low costs. The effects of the modification were evaluated by measuring MW, GP, GE, and CD of the modified starch, as well as sewage TRR and sludge SRF, CST, and WC.

Effects of starch degradation degree on the MW, GP, and GE of starch-*g*-p(DMDAAC) as well as TRR, WC, SRF, and CST are shown in Table 1. The M_w and M_n of starch decreased rapidly, with an increase of degradation time from 30 to 150 min, and then the decrease became moderate. Meanwhile, GP, GE, and CD increased rapidly prior to 150 min, and then reached a plateau value. The results indicate that the grafting polymerization is easy to carry out with a smaller MW. The TRR increased until 150 min and then decreased. The TRR was used to evaluate flocculation capacity. The results indicate that the cationic starch has an optimum flocculation effect when M_w and M_n are 85,136 and 64,496. In contrast, the WC, SRF, and CST had a decreasing tendency with increasing degradation time, and reached a minimum when M_w and M_n are 35,316 and 29,186. Generally, a lower WC and SRF or shorter CST indicates stronger sludge dewaterability. The results demonstrate that starch-*g*-p(DMDAAC) with a larger MW could exhibit good bridging flocculation capacity, while starch-*g*-p(DMDAAC) with a slightly smaller MW has strong sludge dewaterability. The results demonstrate that the degradation degree played a more important role in the flocculation effects and dewaterability of starch-*g*-p(DMDAAC).

3.1.2. DMDAAC content

The degradation starch with an M_w of 35,316 was selected to form a graft copolymer with different amounts of DMDAAC. Other process conditions were kept the same as in Section 3.1.1. Effects of DMDAAC content on MW, GP, GE, TRR, WC, SRF, and CST are shown in Table 2. The results indicate that the TRR increased with increasing DMDAAC content, while WC, SRF, and CST showed minimum values at a DMDAAC content of 25 g. The reason is that flocculation mainly relies on adsorption and bridging for the formation of large and heavy flocs, and more DMDAAC content produces strong cationic groups, which is beneficial for adsorption and bridging flocs. In contrast, the sludge dewaterability mainly relies on strong hydrophobic regions and cationic charge, so the cationic starch should have both stronger hydrophobic groups and cationic groups based on meeting solubility requirements. The results indicate that a suitable DMDAAC content is the key to form strong hydrophobic regions and cationic groups for building a porous structure inside the sludge to be dewatered.

3.1.3. HRP content

Except for HRP content increasing from 2 mg to 4, 6, 8, 10, 12, 14, 16, 18, and 20 mg, respectively, other conditions remained unchanged. The effects of HRP content on GP, GE, TRR, DR, SRF, and CST are shown in Fig. 1. The results indicate that the maximum of GP, GE, and DR appeared at HRP content of 12 mg, and the related WC also reached a minimum value (Fig. 1a). Meanwhile, SRF and CST decreased distinctly with increasing HRP content up to 12 mg. These results indicated that the suitable HRP content is 12 mg for synthesis of the sludge dewatering agent.

In summary, starch-*g*-p(DMDAAC) suitable for sludge dewatering was prepared by graft copolymerization of 25 g of degraded starch and 25 g of DMDAAC using 12 mg of HRP and 15 g of H_2O_2 (30%) at 45 °C for 6 h.

3.2. Molecular structure of starch-*g*-p(DMDAAC)

The FTIR spectra of starch and starch-*g*-p(DMDAAC) are shown in Fig. 2a. The FTIR spectrum of starch is analyzed as follows: 3440 cm^{-1} (—OH), 2935, 1640 cm^{-1} (stretching vibration absorption C—H of —CH_2OH and —CHOH), 1460, 1420, 1373 cm^{-1} (bending vibration absorption C—H of —CH_2OH and —CHOH), 1160, 1080, 1020, 928, 862 cm^{-1} (six-membered ring of starch and C—O—C). The characteristic absorption peaks of starch-*g*-p(DMDAAC) are analyzed as follows: 3400 cm^{-1} (OH), 2930, 2852, 1640 cm^{-1} (stretching vibration absorption C—H of —CH_2OH and —CHOH), 2090 cm^{-1} (characteristic absorption peak of quaternary ammonium salt), 1370, 1224, 1110 cm^{-1} (C—N, C—O—C). The difference between the FTIR spectra of starch and starch-*g*-p(DMDAAC) is obvious. In the FTIR spectrum of starch, there are strong broad absorption peaks at about 3400, 2935, 1640, and 1020 cm^{-1}, which are attributed to —OH, CH_2—, —CH—, and C—O—C. By comparison, the characteristic absorption peaks of —CH_3 (2930, 2852, 1640 cm^{-1}) and C—N (2090, 1224 cm^{-1}) appear in the FTIR spectrum of

Table 2
Effect of DMDAAC content on properties of starch-*g*-p(DMDAAC).

DMDAAC (g)	Molecular weight (Da)			GP (%)	GE (%)	CD (%)	TRR[a] (%)	WC[a] (%)	SRF[a] (10^{13} m kg^{-1})	CST[a] (s)
	M_n	M_w	PDI							
0	29,186	35,316	1.21	–	–	–	45.3	96.3	7.18	72.26
15	29,222	35,358	1.21	177.4	91.25	35.85	73.5	76.4	4.02	51.23
20	29,235	35,374	1.21	177.3	91.13	42.50	95.5	63.3	1.21	28.6
25	29,505	35,406	1.20	178.9	94.63	48.11	95.4	50.1	0.63	11.35
30	29,774	35,431	1.19	178.5	96.13	55.12	95.6	50.5	0.68	11.82
35	29,543	35,452	1.20	177.2	92.57	46.36	95.8	52.7	0.72	12.64

[a] The dosage was 0.6% by solid contaminant weight.

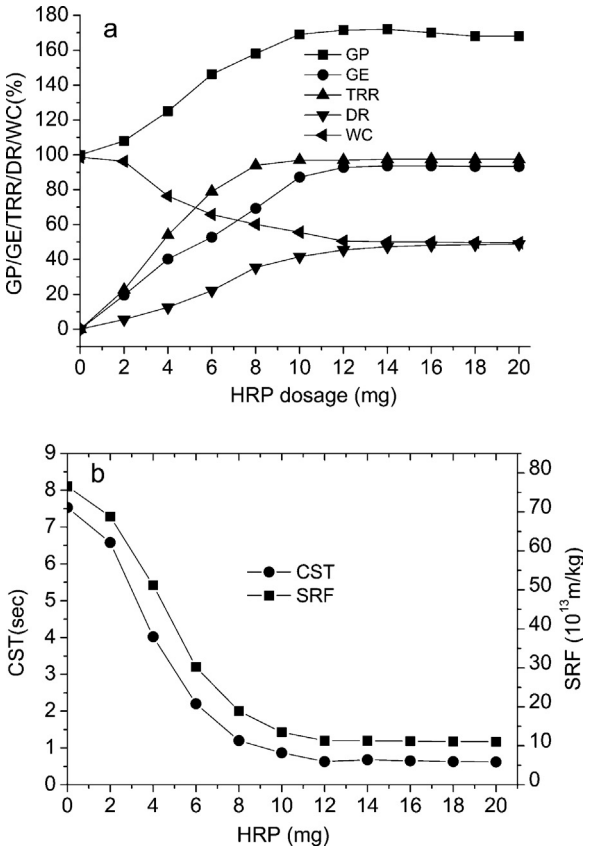

Fig. 1. Effects of HRP content on (a) GP, GE, TRR, DR, and WC and on (b) SRF and CST (the dosage of starch-*g*-p(DMDAAC) was 0.6% by solid sludge weight).

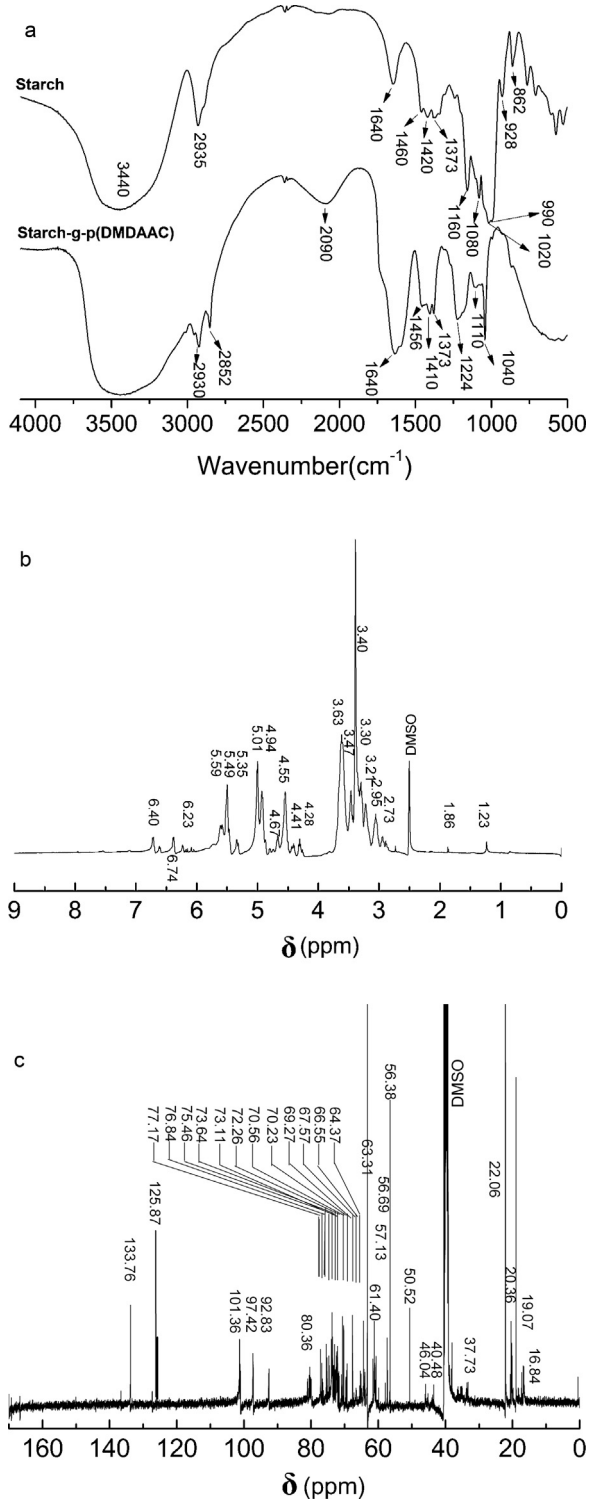

Fig. 2. FTIR spectra of starch and starch-*g*-p(DMDAAC) (a), ^{1}H NMR spectrum (b), and ^{13}C NMR spectrum (c) of starch-*g*-p(DMDAAC).

starch-*g*-p(DMDAAC). Thus, comparison of the FTIR spectra proves that DMDAAC has been grafted onto the starch skeleton.

Analyses of the ^{1}H NMR and ^{13}C NMR spectra of starch-*g*-p(DMDAAC) are required to determine its chemical structure. The spectra are shown in Fig. 2b and c. The spectra are analyzed as follows. ^{1}H NMR (400 MHz, DMSO; δ, ppm): 6.74, 6.40, 6.23, 5.59, 5.49, 5.35, 5.01, 4.94, 4.67, 4.55, 4.41, 4.28, 3.63, 3.47, 3.40, 3.30, 3.21, 3.05, 2.95, 2.74, 1.86, 1.23. ^{13}C NMR (400 MHz, DMSO; δ, ppm): 133.76, 125.87, 101.36, 97.42, 92.83, 80.36, 77.17, 76.84, 75.46, 73.64, 73.11, 70.65, 70.23, 69.27, 67.57, 66.55, 64.37, 63.37, 61.40, 57.13, 56.38, 50.52, 46.04, 40.48, 37.73, 20.36, 22.06, 19.07, 16.84. The chemical structure of starch-*g*-p(DMDAAC) may be determined by comparing the experimental data with the calculated data of the possible chemical structures.

According to the initiation mechanism of HRP/H_2O_2 (Lv et al., 2012; McLean, Agarwal, Atack, & Richardson, 2011) and DMDAAC properties, the synthesis mechanism and the possible structures are presented in Fig. 3. DMDAAC can only form oligomers of five- or six-membered rings ($m < 10$) due to the autoinhibition. The graft polymerization mainly consists of initiation (Fig. 3a), radical transfer, and radical coupling of starch and oligomer (Fig. 3b). The numbering method of H and C is shown in Fig. 3c. The chemical shifts of all H and C can be calculated from

$$\delta_H = 0.23 + \sum \delta_i \quad (7)$$

where δ_H is the shield constant of H; and

$$\delta_C = -2.5 + \sum A_n \quad (8)$$

where δ_C is the shield constant of C, −2.5 is the chemical shift of methane carbon, A is the additional displacement parameter, and n is the number of C atoms with the same additional displacement parameter.

The chemical shifts of H and C of the possible structures of starch-*g*-p(DMDAAC) (labeled 'a' to 'f' in Fig. 3b) are listed as follows:

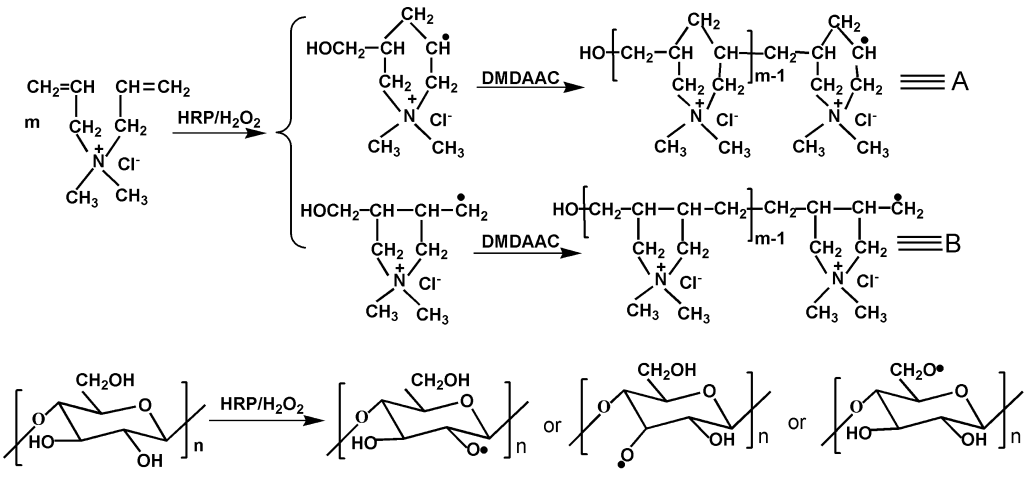

(a) The reaction mechanism of graft copolymerization

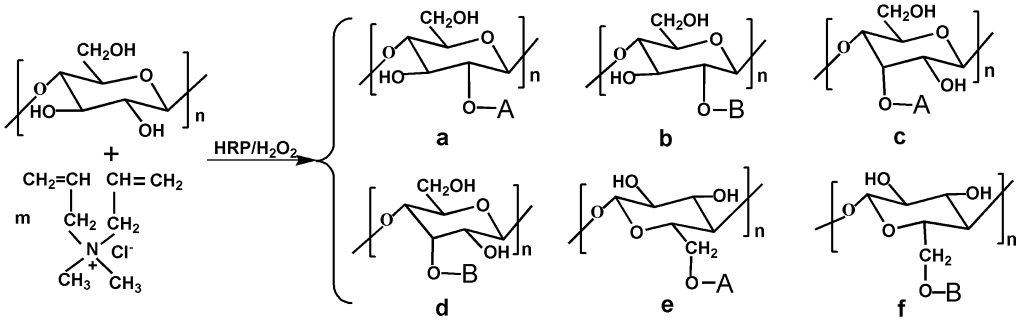

(b) The possible chemical structures of starch-*g*-p(DMDAAC)

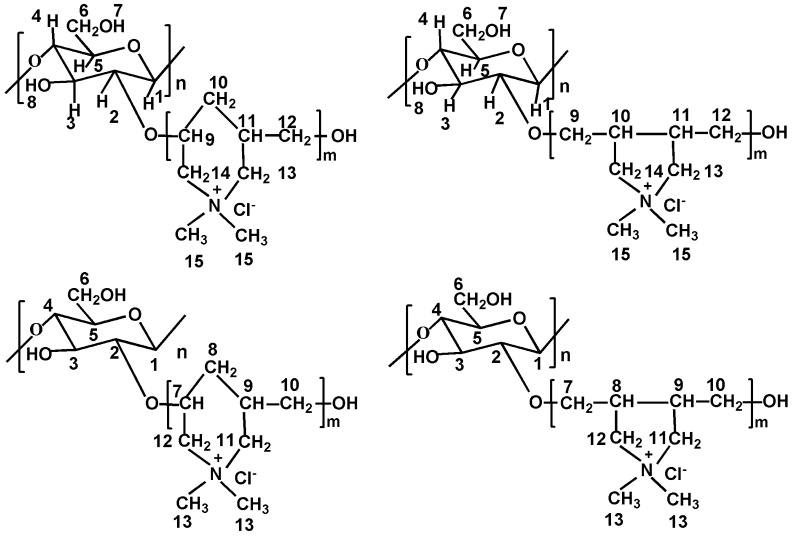

(c) The numbering method of H and C in starch-*g*-p(DMDAAC)

Fig. 3. Synthesis mechanism and the possible structures of starch-*g*-p(DMDAAC).

a: ^{1}**H NMR** (δ, ppm): 6.71 (H1), 6.46 (H2), 4.71 (H3), 4.59 (H4), 3.63 (H6), 3.59 (H5, H9), 3.50 (H14), 3.23 (H10), 2.96 (H7), 2.73 (H11), 2.56 (H8), 2.30 (H13), 1.80 (H15), 1.23 (H12).
^{13}**C NMR** (δ, ppm): 133.12 (C1), 87.63 (C2), 73.26 (C3), 84.11 (C5), 83.22 (C4), 76.46 (C7), 67.25 (C6), 52.07 (C11), 50.13 (C12), 37.43 (C9), 35.23 (C10), 32.42 (C8), 28.53 (C13).

b: ^{1}**H NMR** (δ, ppm): 7.71 (H3), 6.71 (H1), 6.46 (H2), 4.59 (H4, H5), 3.63 (H6), 3.50 (H14), 3.29 (H9), 3.21 (H12), 2.96 (H7), 2.56 (H8), 2.30 (H13), 2.23 (H10), 1.80 (H15).1.73 (H11).
^{13}**C NMR** (δ, ppm): 133.12 (C1), 87.63 (C2), 84.11 (C5), 83.22 (C4), 73.26 (C3), 71.46 (C7), 67.25 (C6), 49.51 (C11), 47.72 (C12), 47.45 (C8), 45.16 (C9), 28.53 (C13), 27.23 (C10).

c: ^{1}**H NMR** (δ, ppm): 6.71 (H1), 6.20 (H2), 5.59 (H3), 5.03 (H4), 3.59 (H5), 3.50 (H14), 3.29 (H6), 3.26 (H9,H10), 2.96 (H7), 2.56 (H8), 2.73 (H11), 2.30 (H13), 1.80 (H15), 1.23 (H12).
^{13}**C NMR** (δ, ppm): 130.83 (C1), 88.04 (C3), 89.92 (C5), 83.06 (C4), 76.43 (C7), 74.92 (C2), 55.81 (C6), 52.07 (C11), 50.12 (C12), 37.43 (C9), 35.25 (C10), 32.43 (C8), 28.53 (C13).
d: ^{1}**H NMR** (δ, ppm): 6.53 (H1), 6.20 (H2), 5.34 (H3), 3.59 (H4, H5), 3.50 (H14), 3.39 (H9), 3.29 (H6), 2.6 (H7, H8), 2.73 (H10), 2.30 (H13), 1.80 (H15), 1.73 (H11), 1.23 (H12).
^{13}**C NMR** (δ, ppm): 130.83 (C1), 88.04 (C3), 83.06 (C4), 82.92 (C5), 55.81 (C6), 74.92 (C2), 71.75 (C7), 49.52 (C11), 47.46 (C8), 47.71 (C12), 45.13 (C9), 28.53 (C13), 27.25 (C10).
e: ^{1}**H NMR** (δ, ppm): 5.41 (H1), 4.52 (H9), 4.29 (H3), 3.83 (H4, H5), 3.76 (H2), 3.50 (H14), 3.33 (H6), 2.56 (H7,H8), 2.30 (H13), 1.80 (H15), 1.73 (H11), 1.23 (H10, H12).
^{13}**C NMR** (δ, ppm): 123.75 (C1), 87.16 (C4), 78.93 (C5), 76.93 (C2), 76.45 (C7), 75.81 (C6), 74.42 (C3), 52.08 (C11), 50.13 (C12), 35.26 (C10), 37.43 (C9), 32.42 (C8), 28.53 (C13).
f: ^{1}**H NMR** (δ, ppm): 5.41 (H1), 3.83 (H4, H5), 3.76 (H2,H3), 3.50 (H14), 3.33 (H6), 2.56 (H7, H8), 2.30 (H13), 1.80 (H15), 1.73 (H10, H11), 1.23 (H12).
^{13}**C NMR** (δ, ppm): 123.75 (C1), 87.16 (C4), 78.93 (C5), 76.93 (C2), 75.81 (C6), 74.42 (C3), 71.43 (C7), 48.97 (C11), 47.78 (C12), 47.46 (C8), 45.13 (C9), 28.53 (C13), 27.23 (C10).

Then, the chemical structure of starch-*g*-p(DMDAAC) may be obtained by comparing the experimental data and the calculated data of all H and C chemical shifts. The chemical shifts of H7, H8, H9, and H10, as well as C7, C8, C9, C10, C11, and C12, proved the presence of the five- and six-membered rings of DMDAAC units. Meanwhile, the shift parameters of H2, H3, and H6, as well as C2, C3, and C6, indicated that the starch-*g*-p(DMDAAC) at least contained the structural units of a, b, c, d, e, and f. The C1 shift parameters of e and f are more than those of the other structures, indicating that e and f are the main products due to steric hindrance.

3.3. Dewatering mechanism of starch-g-p(DMDAAC)

The dewatering mechanism is proposed from analysis of the results of surface tension, zeta potential of sludge, and the microstructure of the dewatered sludge.

3.3.1. Analysis of surface tension of solution

The surface tension of starch-*g*-p(DMDAAC) solution of various concentrations is shown in Fig. 4a. The results indicate that starch-*g*-p(DMDAAC) has stronger surface activity than starch-*g*-p(AM-*co*-DMDAAC) and p(AM-*co*-DMDAAC). Its critical micellar concentration is 1.68×10^{-4} mol L^{-1} and the minimum surface tension is 42.6 mN m^{-1}. Generally, the surface tension depends on molecular structure, especially hydrophilic and hydrophobic groups. The results suggest that there are balanced hydrophobic groups and hydrophilic groups in starch-*g*-p(DMDAAC), where the hydrophobic groups are the alkane structure of DMDAAC and the hydrophobic alkane groups can form larger hydrophobic regions. For poly(AM-*co*-DMDAAC) and starch-*g*-p(AM-*co*-DMDAAC), the hydrophobic alkane groups are separated by hydrophilic AM units, resulting in poor hydrophobicity. The result implies that the synthetic molecular structure conforms with the designed molecular structure.

3.3.2. Analysis of zeta potential of sludge

The zeta potentials of sludge conditioned with the different cationic dewatering agents are shown in Fig. 4b. The results indicate that the addition of cationic dewatering agent can change the negative zeta potential of sludge particles to a positive value. The addition of starch-*g*-p(DMDAAC) into sludge can cause the sludge particles to have a greater positive zeta potential than when p(AM-*co*-DMDAAC) and starch-*g*-p(AM-*co*-DMDAAC) are added. The maximum zeta potential appeared at 0.4% dosage, and the dosage of the maximum zeta potential was exactly consistent with that of the optimum sludge dewatering ratio.

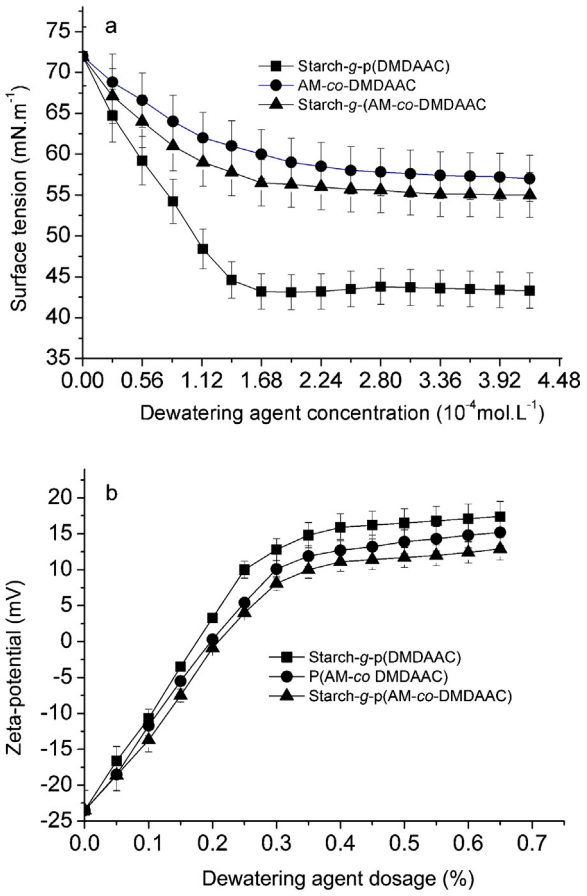

Fig. 4. Surface tension of solution (a) and zeta potential of sludge (b) with starch-*g*-p(DMDAAC).

The reason may be that the sludge particles with higher zeta potential can produce strong repulsion to avoid the formation of gelatinous sludge that makes dewatering very difficult. The results suggest that the sludge dewatering mechanism is different from that of sewage flocculation. Flocculation mainly depends on adsorption and bridging effects to form large and heavy flocs, so sludge with neutral zeta potential as a result of addition of cationic flocculants is beneficial for forming heavy flocs for solid/liquid separation. Sludge dewaterability mainly relies on the formation of hydrophobic sludge particles and porous structure through the addition of a suitable dewatering agent. The starch-*g*-p(DMDAAC) has strong hydrophobic groups and cationic groups, which can help in the formation of hydrophobic regions and porous structure within sewage sludge, leading to easy dewatering.

3.3.3. Analysis of microstructure of dewatered sludge

The effect of starch-*g*-p(DMDAAC) on the microstructure of the dewatered sludge can be assessed by analysis of pore structure and SEM images.

The pore structure of sludge conditioned with the different dewatering agents is shown in Table 3. The results indicate that the dewatered sludge treated with the starch-*g*-p(DMDAAC) has a greater total intrusion volume of mercury and a greater total pore area, as well as a smaller and more uniform pore diameter than that treated with the control samples. The results suggest

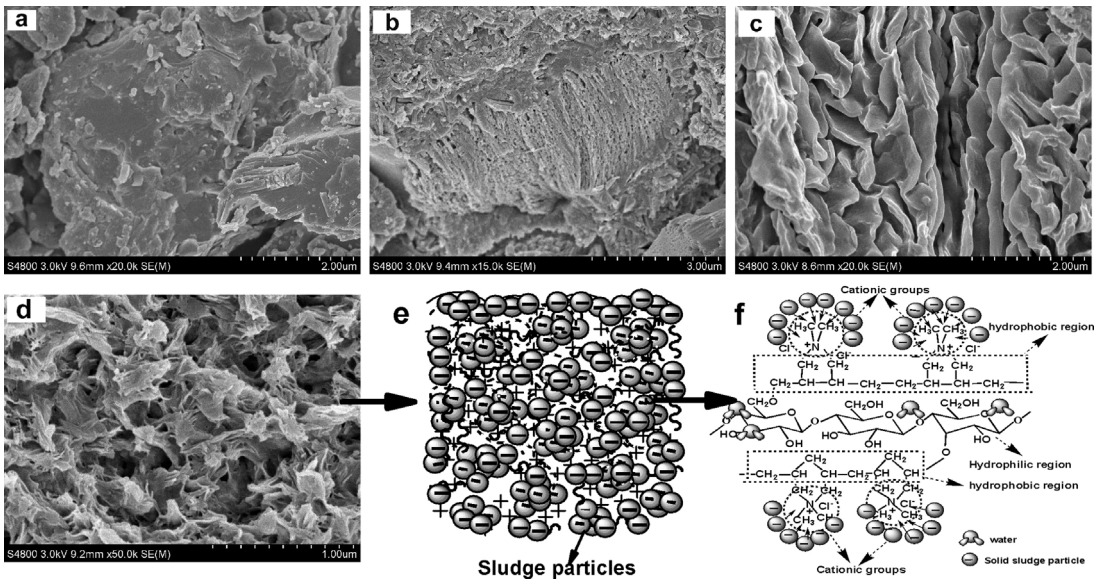

Fig. 5. (a) SEM image of original sludge. SEM images of dewatered sludge conditioned with (b) 0.6% CPAM, (c) 0.6% starch-*g*-p(AM-*co*-DMDAAC), and (d) 0.6% starch-*g*-p(DMDAAC). Schematic diagrams of (e) sludge dewatering mechanism and (f) hydrophobic regions of starch-*g*-p(DMDAAC).

that starch-*g*-p(DMDAAC) has a stronger coagulation and water-repellent capacity within the sludge. Therefore, the more porous structure formed inside the sludge results in a strong dehydration effect, which should be attributed to the special structure of the starch-*g*-p(DMDAAC).

SEM images of the dewatered sludge are shown in Fig. 5. The SEM images indicate that the original sludge has a compact structure (Fig. 5a). The sludge treated with CPAM exhibits a slightly looser structure with small pores (Fig. 5b). By contrast, starch-*g*-p(AM-*co*-DMDAAC) can produce large pores and gaps inside the sludge (Fig. 5c). More particularly, starch-*g*-p(DMDAAC) can form a three-dimensional network porous structure (Fig. 5d). The results indicate that the dewatering mechanism of starch-*g*-p(DMDAAC) is clearly distinguished from that of the control samples, with the predominant feature being the formation of a porous structure, which is closely related to the special structure of starch-*g*-p(DMDAAC) with strong hydrophobic regions and strong cationic groups.

From the discussion above, a possible sludge dewatering mechanism for the starch-*g*-p(DMDAAC) can be proposed, as shown in Fig. 5e. The mechanism may be considered to consist of adsorption, coagulation, and dehydration processes, with the formation of a porous structure that is beneficial to the dewatering process. The dewatering mechanism is exactly opposite to the flocculation mechanism, which mainly depends on hydrophobic groups and regions, as well as stronger cationic groups. The intramolecular cationic and hydrophobic groups of starch-*g*-p(DMDAAC) may weaken the interaction of both intramolecular and intermolecular chains, resulting in low viscosity and high surface activity, as well as better permeation and dispersion in sludge (Anthony & Sims, 2013; Zhang et al., 2007). Then, starch-*g*-p(DMDAAC) will produce strong coagulation or flocculation in sewage sludge as a result of the strong cationic charge. Meanwhile, many cationic branched chains wrap around the long starch backbone and form a cationic charge shield, weakening the hydrogel-forming capacity. The hydrophobic groups may be connected to form intramolecular hydrophobic regions (Fig. 5f), which is beneficial for the formation of a hydrophobic pore structure. The starch-*g*-p(DMMDAC) suitable for sludge dewatering has a smaller molecular weight (shorter polymer chain length) compared with the same structural flocculant. The formation of the porous structure with interpenetration inside the sludge is a synergistic effect of hydrophobic and hydrophilic regions, as well as cationic groups in starch-*g*-p(DMDAAC), which is beneficial to sludge dehydration.

Table 3
The pore structure of the dewatered sludge.

	Starch-*g*-p(DMDAAC)	CPAM	Starch-*g*-p(AM-*co*-DMDAAC)
Dosage (%)	0.6	0.6	0.6
Total intrusion volume (mL g^{-1})	0.135	0.069	0.108
Total pore area (m^2 g^{-1})	25.16	12.60	17.05
Median pore diameter (volume) (nm)	25.3	26.1	31.2
Median pore diameter (area) (nm)	19.6	12.6	23.2
Average diameter (4 V/A) (nm)	25.8	31.9	26.5
Bulk density at 3.86 kPa (g mL^{-1})	1.85	2.00	1.85
Apparent density (g mL^{-1})	1.83	2.12	1.98
Porosity (%)	42.74	13.84	21.80

4. Conclusions

Starch-*g*-p(DMDAAC) was synthesized by graft copolymerization of 25 g of degradation starch and 25 g of DMDAAC using HRP (12 mg)/H_2O_2 (15 mL) initiation at 45 °C for 6 h. The results of FTIR, ^{1}H NMR, and ^{13}C NMR indicated that the molecules of the starch-*g*-p(DMDAAC) were built by grafting shorter branched chains of oligomeric DMDAAC, with this oligomer consisting of a five- and six-membered ring-like structural unit. The special feature of the chemical structure is that there are stronger hydrophobic regions and cationic degree in the starch-*g*-p(DMDAAC) molecules, which is beneficial for improving sludge dewaterability, with the CST and the SRF reduced markedly compared with the original sludge. The excellent dewatering effect was attributed to the special molecular structure. The dewatering mechanism is proposed based on results of the surface activity and the zeta potential of starch-*g*-p(DMDAAC), as well as on the analysis of pore structure and SEM images of the dewatered sludge. The molecular design and synthesis method involved in the study reported in this paper are

of significance for the development of high-performance sludge dewatering agents from starch, a natural resource.

Acknowledgment

We thank the Natural Science Foundation of China (20876091, 21076121) for financial support for this research.

References

Ali, P., Seyed, M. F., & Seyed, H. H. (2013). Novel cationic-modified salep as an efficient flocculating agent for settling of cement slurries. *Carbohydrate Polymers*, *93*, 506–511.

Anthony, R. J., & Sims, R. C. (2013). Optimization of cationic amino starch synthesis using biogenic amines. *Carbohydrate Polymers*, *98*, 1409–1415.

Kavaliauskaite, R., Klimaviciute, R., & Zemaitaitis, R. (2008). Factors influencing production of cationic starches. *Carbohydrate Polymers*, *73*, 665–675.

Krentz, D. O., Lohmann, C., Schwarz, S., Bratskaya, S., Liebert, T., & Laube, J. (2006). Properties and flocculation efficiency of highly cationized starch derivatives. *Starch/Stärke*, *58*, 161–169.

Kriz, A. J., Dybal, J., & Kurkova, D. (2002). Cooperative counterion–polyion interactions in polyelectrolyte chain dynamics: NMR and quantum-chemical study of locally collapsed state in dilute poly(N-diallyl dimethyl ammonium chloride) in $NaCl/D_2O$ solutions. *Journal of Physical Chemistry A*, *106*, 7971–7981.

Lin, Q., Qian, S., Li, C., Pan, H., Wu, Z., & Liu, G. (2012). Synthesis, flocculation and adsorption performance of amphoteric starch. *Carbohydrate Polymers*, *90*, 275–283.

Lu, M. C., Lin, C. J., Liao, C. H., Huang, R. Y., & Ting, W. P. (2003). Dewatering of activated sludge by Fenton's reagent. *Advances in Environmental Research*, *7*(3), 667–670.

Lv, S. H., Gong, R., & Ma, Y. F. (2012). Structure and properties of the graft copolymer of starch and p-hydroxybenzoic acid using horseradish peroxidase. *Polymer for Advanced Technologies*, *23*(10), 1343–1349.

Lv, X. H., Song, W. Q., Ti, Y. Z., Qu, L. B., Zhao, Z. H., & Zheng, H. J. (2013). Gamma radiation-induced grafting of acrylamide and dimethyl diallyl ammonium chloride on to starch. *Carbohydrate Polymers*, *92*, 388–393.

Ma, J. Y., Zheng, H. L., Tan, M. Z., Liu, L. W., Chen, W., Guan, Q. Q., et al. (2013). Synthesis, characterization, and flocculation performance of anionic polyacrylamide P(AM-AA-AMPS). *Journal of Applied Polymer Science*, *129*(4), 1984–1991.

McLean, D., Agarwal, V., Stack, K., Horne, J., & Richardson, D. (2011). Synthesis of guar gum-graft-poly(acrylamide-co-dimethyl diallyl ammonium chloride) and its application in the pulp and paper industry. *BioResources*, *6*, 4168–4180.

Mishra, S., Mukul, A., Sen, G., & Jha, U. (2011). Microwave assisted synthesis of polyacrylamide grafted starch (St-g-PAM) and its applicability as flocculant for water treatment. *International Journal of Biological Macromolecules*, *48*, 106–111.

Noppakundilograt, S., Nanakorn, P., Jinsart, W., & Kiatkamjornwong, S. (2010). Synthesis of acrylamide/acrylic acid-based aluminum flocculant for dye reduction and textile wastewater treatment. *Polymer Engineering and Science*, *50*(8), 1535–1546.

Ochoa, J. R., Escudero Sanz, F. J., Sasia, P. M., Santos García, A., Díaz de Apodaca, E., & Río, P. (2007). Synthesis of cationic flocculants by the inverse microemulsion copolymerization of acrylamide. *Journal of Applied Polymer Science*, *203*(1), 186–197.

O'Shea, J.-P., Qiao, G. G., & Franks, G. V. (2011). Temperature responsive flocculation and solid–liquid separations with charged random copolymers of poly(N-isopropyl acrylamide). *Journal of Colloid and Interface Science*, *360*(1), 61–70.

Pal, S., Sen, G., Karmakar, N. C., Mal, D., & Singh, R. P. (2008). High performance flocculating agents based on cationic polysaccharides in relation to coal fine suspension. *Carbohydrate Polymers*, *74*, 590–596.

Randal, L., & Shogren, A. B. (2013). Preparation of starch–sodium lignosulfonate graft copolymers via laccase catalysis and characterization of antioxidant activity. *Carbohydrate Polymers*, *91*, 581–585.

Tawaki, S. C., Uchida, Y. G., Maeda, Y. S., & Ikeda, I. (2005). HRP-catalyzed polymerization of sugar-based phenols in aqueous organic solvents. *Carbohydrate Polymers*, *59*, 71–74.

Wang, J. P., Chen, Y. Z., Wang, Y., Yuan, S. J., Sheng, G. P., & Yu, H. Q. (2012). A novel efficient cationic flocculant prepared through grafting two monomers onto chitosan induced by Gamma radiation. *RSC Advances*, *2*(2), 494–500.

Wang, Y. B., & Xie, W. L. (2010). Synthesis of cationic starch with a high degree of substitution in an ionic liquid. *Carbohydrate Polymers*, *80*, 1172–1177.

Zhang, M., Ju, B. Z., Zhang, S. F., Ma, W., & Yang, J. Z. (2007). Synthesis of cationic hydrolyzed starch with high DS by dry process and use in salt-free dyeing. *Carbohydrate Polymers*, *69*, 123–129.

Zou, C. J., Zhao, P. W., Ge, J., Lei, Y., & Luo, P. Y. (2012). β-Cyclodextrin modified anionic and cationic acrylamide polymers for enhancing oil recovery. *Carbohydrate Polymers*, *87*, 607–613.